

CHROM. 18 881

## CHARACTERIZATION OF INTERNAL SURFACE REVERSED-PHASE SILICA SUPPORTS FOR LIQUID CHROMATOGRAPHY

STEVEN E. COOK and THOMAS C. PINKERTON\*

*Department of Chemistry, Purdue University, West Lafayette, IN 47907 (U.S.A.)*

(Received May 29th, 1986)

---

### SUMMARY

Internal surface reversed-phase (ISRP) supports synthesized from commercially available porous silica particles with a variety of nominal pore diameters and specific surface areas are characterized with regard to physical and chromatographic properties. Bonded phase coverage, pore size, capacity and efficiency measurements are made upon the various ISRP supports in order to evaluate the effect that the physical properties of silica have upon the chromatographic performance of ISRP packings. In addition, various models that describe the pore structure of silica supports are discussed.

---

### INTRODUCTION

Recent reports have described the production of internal surface reversed-phase (ISRP) liquid chromatographic (LC) packing materials for use in the separation and quantification of small hydrophobic drugs and metabolites in protein containing matrices such as blood serum<sup>1,2</sup>. The ISRP supports allow for the direct injection of serum samples onto the chromatographic column, thus eliminating time-consuming preparation required to rid samples of the proteins that can clog pores and interfere with the quality of separations in conventional RPLC<sup>3,4</sup>. ISRP packing materials are unique in that the hydrophobic partitioning phase is present only on the internal surfaces of the porous silica supports, while a hydrophilic phase, which is non-adsorptive to proteins, covers the external surfaces. Serum proteins, being too large to enter into the pores of the support, "see" only the non-adsorptive hydrophilic external phase and elute rapidly in the interstitial void volume. The small hydrophobic analytes, on the other hand, can penetrate into the porous interior of the support and interact with the partitioning phase.

Two methods for producing ISRP supports have been described<sup>1,2</sup>. The first involves binding a hydrophobic glycyl-L-phenylalanyl-L-phenylalanine (Gly-L-Phe-L-Phe) tripeptide to the surface of glycerolpropyl-bonded porous silica particles. This is followed by enzymatic cleavage of the phenylalanine moieties on the external surface via carboxypeptidase A. In the second method, a butoxy-L-phenylalanine (Boc-L-Phe) partitioning phase is bound to an alkylamine-bonded silica support.  $\alpha$ -Chy-

motrypsin is then utilized to cleave the Boc-L-Phe phase from the external surface, and the remaining external residual alkylamine groups are capped with glycidol. While both methods result in functional ISRP supports with a hydrophobic phenyl-alanine internal partitioning phase and a non-adsorptive glycerolpropyl external phase, the carboxypeptidase method of ISRP synthesis is that which has been commercialized (Pinkerton ISRP columns by the Regis Chemical Company) and is predominantly investigated in our research.

In the ISRP supports produced by the enzymatic cleavage methods, the fraction of total surface area which is considered to be internal or external surface is dependent upon the size of the cleavage enzyme molecule and the pore structure of the silica support. Pores in a specific porous silica material are not of uniform size, but can be described by a narrow pore size distribution. Surfaces existing within pores that allow access of cleavage enzyme molecules with proper orientation will be cleaved and will be considered external surface. Relative to small pore supports, large pore silicas will allow greater access of the cleavage enzyme to the support surface and will yield a smaller internal surface and less capacity for the hydrophobic analytes. This trend is compounded by the fact that larger pore silicas generally have less specific surface area than the smaller pore supports<sup>5,6</sup>. From this brief discussion, it might be assumed that a silica support with small pore diameters and high specific surface area would be ideal for production of an ISRP material exhibiting a large percent internal surface and high capacity. However, because of the extensive chemical derivatization associated with the production of the ISRP packings, the pores of small pore silicas may be closed to the extent that diffusional mass transfer of analyte into the porous support interior becomes inhibited; thus detrimentally affecting the efficiency of separations<sup>7-9</sup>. It is important, therefore, to take care in selecting the initial porous silica for ISRP synthesis so that the pore structure of the support is of such a nature to allow maintenance of a significant fraction of internal partitioning phase without exhibiting the loss of chromatographic performance associated with small pores.

The intent of the current work is to characterize, with regard to physical and chromatographic properties, high-performance Gly-L-Phe-L-Phe ISRP supports made from commercially available spherical porous silica of varying pore sizes and surface areas. In doing so, the effects that the physical properties of porous silica supports have upon the chromatographic performance of ISRP packings can be elucidated.

#### PORE STRUCTURE OF SPHERICAL POROUS SILICA

Spherical porous silica particles with diameters in the order of 3–10  $\mu\text{m}$  are typically used as support packings in high-performance liquid chromatography (HPLC) today. The porous silicas are made through the agglomeration of tiny non-porous silica microspheres<sup>10,11</sup>. The pores in the support particles are created by the space between the agglomerated colloidal microspheres, and therefore, the structural characteristics (*i.e.*, surface area, pore size and shape) of the support depend upon the size and packing density of the microspheres. Models have been developed to describe the structure of the microsphere agglomerates and the resulting pore structure of the silica. Briefly explained below are three of these models.

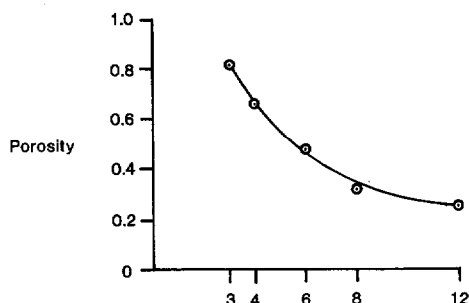


Fig. 1. Porosity dependence on contact number of microspheres for porous objects.

*Globular model.* The globular model for porous objects developed by Karnaukhov<sup>12,13</sup> utilizes uniform size microspheres which can agglomerate with any integral or fractional value of contact number ( $n$ ) from 3 to 12. Two fundamental equations are derived which relate the specific surface area ( $S$ ), specific pore volume ( $V$ ), and pore neck diameter ( $d$ ) of the porous materials made from microspheres with diameter,  $D$ . The first relationship allows for the calculation of specific surface area from the diameter of the microspheres.

$$S = \frac{6}{\delta D} \quad (1)$$

where  $\delta$  is the density of the pure solid microspheres (approximately 2.2 g/cm<sup>3</sup> for silica). The second relationship results from the assumption that the pores are approximately cylindrical in shape. It takes the form of the equation that describes perfect cylinders.

$$d = \frac{\gamma V}{S} \quad (2)$$

where the packing coefficient ( $\gamma$ ) is calculated to have an average value of 2.8 for randomly packed microspheres. The relationship between the specific pore volume of a porous material and its porosity ( $P$ ) is represented in eqn. 3, while Fig. 1 shows the exclusive dependence of porosity on the contact number of the microspheres.

$$P = \frac{V}{V + 1/\delta} \quad (3)$$

Unger *et al.*<sup>10</sup> have previously discussed this globular model and its relationship to spherical porous silica particles. In principle, if the packing density (porosity) and the size or specific surface area of the microspheres are known, then the average pore size for the porous silica can be determined.

*Random sphere model.* The random sphere model (RSM) involves randomly placed microspheres of equal size which are allowed to overlap or imbed into one another<sup>14,15</sup>. This model is similar to the globular model in that knowledge of mi-

TABLE I  
STRUCTURAL CHARACTERISTICS OF COMMERCIAL SILICA PARTICLES

	<i>Hypersil</i>	<i>Nucleosil-100</i>	<i>Spherisorb</i>	<i>Zorbax</i>	<i>Nucleosil-50</i>	
Particle diameter, $d_p$ ( $\mu\text{m}$ )	5	5	5	6	5	
Nominal pore diameter, $d$ ( $\text{\AA}$ )	123	100	80	70	59	
Specific surface area, $S$ ( $\text{m}^2/\text{g}$ )	180	300	220	350	500	
Specific pore volume, $V$ ( $\text{cm}^3/\text{g}$ )	0.67	1.0	—	—	0.8	
Microsphere diameter, $D$ ( $\text{\AA}$ )**	121	78	92	64	48	
Specific pore volume, $V$ ( $\text{cm}^3/\text{g}$ )**	0.82	1.3	0.58	0.95	1.3	
Microsphere diameter, $D$ ( $\text{\AA}$ )***	152	91	124	78	55	
Specific pore volume, $V$ ( $\text{cm}^3/\text{g}$ )§	0.79	1.1	0.63	0.88	1.1	
Porosity, $P^{\S\S}$	0.63	0.71	0.58	0.66	0.71	
Contact number, $n^{\S\S\S}$	4.3	3.7	4.7	4.0	3.7	
						Manufacturer's specifications RSM*
						Globular model*

\* For all calculations  $\delta = 2.2 \text{ g/cm}^3$ .

\*\* Calculated from RSM; eqns. 3–6 and manufacturer specified  $S$  and  $d$ .

\*\*\* Calculated from globular model; eqn. 1 and manufacturer specified  $S$ .

§ Calculated from globular model; eqn. 2 and manufacturer specified  $S$  and  $d$ .

§§ Calculated from eqn. 3 and  $V$  calculated from globular model.

§§§ Determined from Fig. 7, eqn. 3 and  $V$  calculated from globular model.

crossphere size and porosity of the silica will allow the calculation of the average pore size according to eqns. 4 and 5.

$$R_D = \frac{-3P}{S_v} \ln P \quad (4)$$

$$R_d = (1.32 - P) \frac{2P}{S_v} \quad (5)$$

where  $R_D$  is the radius of the solid microspheres,  $P$  is the porosity (eqn. 3),  $R_d$  is the average radius of the pores and  $S_v$  is the surface area per unit volume of the system (eqn. 6).

$$S_v = \frac{S}{V + 1/\delta} \quad (6)$$

Van Kreveld and Van den Hoed<sup>15</sup> have shown that good correlation exists between the determination of the structural characteristics of Porasil silica by this model and experimental data. An advantage of the RSM over the globular model is that the RSM can be used to accurately predict size exclusion chromatographic calibration curves<sup>15,16</sup>.

*Random size touching sphere model.* More recently Knox and Scott<sup>16</sup> have developed an elaborate computer generated random size touching spheres model which overcomes a major criticism of the RSM and globular model: most real porous silica systems may not actually consist of uniform size microspheres. The model of Knox and Scott<sup>16</sup> results in randomly placed, non-overlapping microspheres with sizes chosen randomly from a unimodal gaussian size distribution. This model was developed in order to theoretically predict size exclusion calibration curves, and while it elegantly serves this purpose, it is more complex and computer dependent than previously described simpler models.

In order to compare the random sphere and globular models, specific pore volumes and microsphere diameters were determined from the manufacturer specified surface areas and pore diameters for five commercial porous silicas. Table I includes these values calculated from the two models. In general, for a given silica, calculation of  $V$  from the globular model and RSM result in similar values that show fair agreement with the manufacturer determined  $V$ . The microsphere diameters determined by the globular model are larger and cover a broader range than those of the RSM, but the expected inverse relationship between surface area and microsphere size is clearly illustrated by the values calculated from both models.

To demonstrate the synergistic effect of microsphere size and packing density on the pore size of the silica supports, the contact numbers for the microspheres in each of the commercial silicas were determined, according to the globular model, from Fig. 1. From close examination of the contact numbers and microsphere diameters in Table I, it can be inferred that a specified pore diameter can be achieved by tight packing of large microspheres or loose packing of small microspheres and inversely a given packing density yields pore sizes which are dependent upon microsphere size.

## EXPERIMENTAL

### *Production of ISRP HPLC columns*

ISRP HPLC packings were produced from commercially available spherical porous silica supports with particle diameters of approximately 5  $\mu\text{m}$  (Spherisorb silica, Phase Separations, Hauppauge, NY, U.S.A.; Nucleosil-50 and Nucleosil-100 silica, Macherey-Nagel, Düren, F.R.G.; Zorbax silica, Dupont, Wilmington, DE, U.S.A.; Hypersil silica, Shandon Southern Products, London, U.K.). Nominal pore sizes and surface areas of these silicas, as specified by the manufacturers, ranged from 59 to 123 Å and 180 to 500  $\text{m}^2/\text{g}$ , respectively (Table I). The synthetic procedure for producing the high-performance ISRP supports was similar to that described in the literature<sup>1,17</sup>. Glycerolpropyl groups were covalently bound to the silica supports by silanization with  $\gamma$ -glycidioxypropyltrimethoxysilane; thus rendering the support non-adsorptive to proteins. The glycol groups of the glycolphase supports were activated with carbonyldiimidazole and Gly-L-Phe-L-Phe tripeptides were bound at their N-termini to the glycolphase via carbamate linkages. In an attempt to increase the surface concentration of the partitioning phase, the tripeptide addition reaction was allowed to proceed for 3 1/2 to 5 1/2 days rather than the 2 to 3 days recommended by Pinkerton and Hagestam<sup>17</sup>. The hydrophobic phenylalanine residues of the bound tripeptide phase were then cleaved from the external surfaces of the supports by the enzyme carboxypeptidase A. The internal surfaces of the resulting ISRP packings consisted of hydrophobic Gly-L-Phe-L-Phe moieties; while the external surfaces were hydrophilic and non-adsorptive to proteins. In addition to the laboratory-made supports, glycolphase silica and ISRP packing provided by the Regis Chemical Company (Morton Grove, IL, U.S.A.) were also evaluated in this study.

Selected silica supports were slurry packed into 15 cm  $\times$  4.6 mm I.D. stainless-steel columns with a commercial column packing instrument (Shandon Southern Products) or by the Regis Chemical Company proprietary column packing method. Observations over the duration of the investigation suggested that both methods resulted in "well-packed" columns.

### *Determination of glycerolpropyl group (glycolphase) coverage*

Glycolphase silica was subjected to oxidation with standardized periodic acid solution. The periodic acid remaining after complete oxidation of the glycol groups was determined by titration with thiosulfate in the presence of excess iodide. Glycol phase coverage was then calculated from stoichiometric analysis of the iodometric titration<sup>18</sup>.

### *Determination of tripeptide coverage*

Determination of internal and external surface tripeptide coverage was accomplished by reversed-phase HPLC quantification of phenylalanine residues released by the acid hydrolysis (6 *M* hydrochloric acid for 24 h, at approximately 100°C) of ISRP packing before and after cleavage treatment.

### *Chromatography*

*Apparatus.* Chromatography was performed with the use of an LC system consisting of an LC9533 chromatograph, an LC9523 variable-wavelength detector

set to monitor at 254 nm (IBM, Danbury, CT, U.S.A.) and an HP3390A integrator (Hewlett-Packard, Palo Alto, CA, U.S.A.).

*Chromatographic measurements.* Standard solutions (ca. 0.005% w/v) of the anticonvulsant drug carbamazepine were used to evaluate the capacity and efficiency of HPLC columns packed with ISRP supports. The mobile phase used for elution of carbamazepine through the columns consisted of 0.1 M phosphate buffer-isopropanol-tetrahydrofuran (84:10:6, pH 6.8). Capacity factor measurements were performed at a mobile phase flow-rate of 1 ml/min. Efficiencies ( $N$ ) of the 15-cm chromatographic columns were calculated using eqn. 7.

$$N \text{ (plates/meter)} = \frac{5.54 \left( \frac{t_R}{w_{1/2}} \right)^2}{0.15} \quad (7)$$

where  $t_R$  is the retention time of the carbamazepine standard and  $w_{1/2}$  is the width of the carbamazepine peak at one-half the peak height. Capacity factors ( $k'$ ) were determined from eqn. 8.

$$k' = \frac{t_R}{t_R - t_M} \quad (8)$$

where  $t_M$  is the time for mobile phase molecules to pass through the column. Eqn. 9 was used to calculate the chromatographic flow velocity ( $u$ ) for the plate height *versus* flow velocity plots.

$$u \text{ (cm/s)} = \frac{15 \text{ (cm)}}{t_M \text{ (s)}} \quad (9)$$

In order to make relative measurements of capacity factors and chromatographic flow velocities for comparison between the packed columns, void volume perturbations in the baseline occurring at retention times similar to that of the unsorted solute, uracil, were used for determination of mobile phase elution time ( $t_M$ ).

#### *Pore volume access distributions*

Pore volume access distributions provide information regarding the fraction of pore volume in LC packing to which molecules with a given effective sphere radius have access. Pore volume access distributions are obtained by an inverse size-exclusion chromatographic method that involves measurement of the retention volumes of a series of polystyrene molecular weight standards which are eluted through a chromatographic column with a strong mobile phase such as tetrahydrofuran (THF). The success of the inverse size-exclusion method relies on the fact that the strong organic mobile phase allows retention to occur solely by a size exclusion mechanism rather than by any partitioning of standards with the stationary phase.

In the present study, solutions consisting of individual polystyrene standards (Polysciences, Warrington, PA, U.S.A.) with molecular weights ranging from 300 to 300 000 and benzene as an internal standard were injected onto selected chromato-

graphic columns with a mobile phase of 100% THF at a flow-rate of 0.5 ml/min. The flow-rate was monitored by measuring the time required to collect a specified volume of eluent. The interstitial volumes ( $V_z$ ) of the packed columns were determined by measuring the elution volume of the 300 000 molecular weight polystyrene standard (assumed to be totally excluded from the pores), while the pore volume ( $V_p$ ) of the packings were determined by subtracting  $V_z$  from the elution volume of benzene (assumed to be totally included into the pores).

The pore volume access distributions consisted of plots of the size-exclusion coefficient ( $K_{sec}$ ) versus the effective sphere radius for the polystyrene molecules.  $K_{sec}$  for each polystyrene standard was calculated from eqn. 10.

$$K_{sec} = \frac{V_e - V_z}{V_p} \quad (10)$$

where  $V_e$  is the elution volume of the polystyrene standard of interest. The effective sphere radii of the polystyrene standards in THF ( $r$ ) were calculated from the molecular weights (MW) of the standards according to eqn. 11 (see ref. 16).

$$r(\text{\AA}) = 0.123 \text{ MW}^{0.588} \quad (11)$$

#### *Determination of median pore diameter from pore volume access distributions*

The inverse size-exclusion technique described above is similar to one used by Halász and co-workers<sup>19,20</sup> and others<sup>21,22</sup> for determination of cumulative pore size distributions (PSD) in porous HPLC packings. The cumulative PSDs of Halász and co-workers<sup>19,20</sup> are curves of  $K_{sec}$  (eqn. 10) versus log pore diameter ( $\phi$ ), where the  $\phi$  value associated with the  $K_{sec}$  equal to 0.5 is the median pore diameter of the porous packing of interest. Values of  $\phi$  are calculated from the molecular weights (MW) of polystyrene standards according to an empirically derived relationship<sup>19</sup>.

$$\phi (\text{\AA}) = 0.62 \text{ MW}^{0.59} \quad (12)$$

It has been observed that cumulative PSDs resulting from the Halász method are much broader than those determined by other means<sup>22,16</sup>. This arises because small molecules that are able to enter into a pore of a given size will be accessible to more pore volume than larger molecules that are also small enough to enter the pore. For this reason packing materials with pores of uniform diameter, theoretically, can separate molecules on the basis of size<sup>23</sup>. This was not taken into account in the inverse size-exclusion method of Halász and co-workers<sup>19,20</sup>, and the resulting broad cumulative PSDs may not adequately represent the true pore size distributions of porous packings. However, since eqn. 12 was derived from comparison of PSD maxima for various silicas determined by the Halász method and PSD maxima determined from "classical" methods, median pore sizes (the value of  $\phi$  at  $K_{sec} = 0.5$ ) may be estimated from the Halász PSD plots<sup>19</sup>. The pore volume access distributions described in the present study only differ from the PSDs of Halász by a factor of 5.0 on the abscissa [ $\phi$  (eqn. 12) for polystyrene standards is 5.0 times larger than the effect sphere radius (eqn. 11) of polystyrene standards in THF<sup>19</sup>]; thus median pore



diameters can be estimated from pore volume access distributions also. This is simply done by multiplying by 5.0 the value of  $r$  corresponding to  $K_{\text{sec}} = 0.5$  on the pore volume access plot.

## RESULTS AND DISCUSSION

### *Physical characterization of ISRP supports*

ISRP packings produced from various silica supports exhibit significant differences in their pore volume access distributions (Fig. 2). In general, as expected, the pore volume access plots of ISRP supports made from small pore silica lie to the left of the pore volume access plots of packings made from the larger pore silica. This demonstrates that, in most cases, a molecule of a given size will gain access to a greater fraction of the pore volume in the larger pore materials. Median pore diameters of the ISRP supports determined from pore volume access distributions range from 35 Å for the Zorbax ISRP support to 80 Å for the Hypersil ISRP material (Table II). These pore sizes are 17–43 Å lower than the manufacturer specified nominal pore diameters of the initial silica supports (Table I).

Pore volume access distributions for ISRP packing and glycolphase silica (prior to carbonyldimazole activation) produced by the Regis Chemical Company and the silica brand used to synthesize these packings are shown in Fig. 3. Median pore diameters (Table II) for these materials determined from the plots indicate that derivatization of the base silica support with  $\gamma$ -glycidoxypyriltrimethoxysilane decreases the median pore diameter by 22 Å, while the median pore size is reduced an additional 8 Å by the binding of the hydrophobic tripeptide phase. It is interesting to note that the manufacturer specified median pore diameter (80 Å) of the base silica support agrees well with that value estimated from the inverse size-exclusion method (84 Å).

As described in the introduction, the degree to which the hydrophilic external surface of the ISRP supports extends into the microporous interior depends, partially, on the molecular size of the cleavage enzyme. The carboxypeptidase molecule has been estimated to have an effective sphere radius of 31 Å (ref. 1). From this information and the assumption that the enzyme cleaves all surfaces that surround the

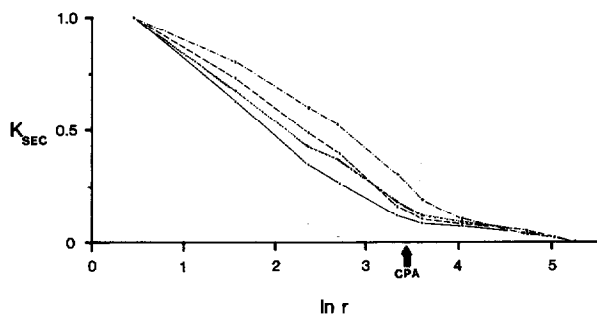


Fig. 2. Pore volume access distributions as determined by inverse size-exclusion chromatography (see Experimental) for various ISRP supports.  $K_{\text{sec}}$  is the size-exclusion coefficient and  $r$  is the effective sphere radius (in Å) of polystyrene standards in THF. The arrow indicates the effective sphere radius of carboxypeptidase A (31 Å). (— · — · —) Hypersil ISRP, batch No. 1; (— — —) Spherisorb ISRP, batch No. 4; (· · · · ·); Nucleosil-50 ISRP, batch No. 1; (—) Zorbax ISRP, batch No. 2.

TABLE II  
STRUCTURAL AND CHROMATOGRAPHIC PROPERTIES OF SELECTED ISRP AND SILICA SUPPORTS

Material	Batch No.	Surface area* (m <sup>2</sup> /g)	Pore diameter** (Å)	k <sub>0</sub> ***	V <sub>p</sub> §	V <sub>z</sub> §§	N§§§ (plates/m)	k' <sup>†</sup>
Nucleosil-50 ISRP	1	500	42	0.59	0.57	0.959	18 400	4.21
Zorbax ISRP	2	350	35	0.44	0.44	1.00	8970	3.34
Spherisorb ISRP	4	220	52	0.50	0.51	1.02	23 600	2.88
Hypersil ISRP	1	180	80	0.61	0.62	1.02	19 500	2.00
Regis Base silica	—	220	84	0.67	0.79	1.03	—	—
Regis glycolphase silica	—	220	62	0.51	0.52	1.01	—	0.85
Regis ISRP	—	220	54	0.49	0.53	1.09	22 000	4.01

\* Specific surface area of initial silica support (manufacturer's value).

\*\* Median pore diameter of support determined from pore volume access distributions.

\*\*\* k<sub>0</sub> = Pore volume/interstitial volume.

§ Pore volume for a 15 cm × 4.6 mm I.D. packed column.

§§ Interstitial volume for 15 cm × 4.6 mm I.D. packed column.

§§§ N is efficiency for carbamazepine in 0.1 M phosphate-isopropanol-tetrahydrofuran (84:10:6, pH 6.8) at 1.0 ml/min, where  $N = 5.54 (t_R/w_{1/2})^2$ ,  $t_R$  is retention time of carbamazepine, and  $w_{1/2}$  is width at one-half maximum peak height.

† Capacity factor of carbamazepine at same conditions as the previous footnote, where  $k' = (t_R - t_M)/t_M$ , and  $t_M$  is elution time of mobile phase.

pore volume to which the carboxypeptidase molecules have access, the fraction of pore volume associated with internal surface and that associated with external surface can be approximated. In fact, if it is assumed that, when compared to the total surface area of the support, the fraction of surface area associated with the interstitial volume of the packed column is negligible, and that the fraction of total pore volume that a molecule has access to is estimated to be proportional to the fraction of total surface area that the molecule can contact, then the percent internal and external surface can be determined from the pore volume access distributions and knowledge of the effective sphere radius of the carboxypeptidase molecule can be obtained. Pore volume access distributions of the ISRP supports (Fig. 2) indicate that the carboxypeptidase molecule has access to 11–26% of the total pore volume, depending on the support, which implies that 74–89% of the total surface area of the supports are hydrophobic internal surface.

#### *Coverage characterization of ISRP supports*

The first step in the synthesis of the Gly-L-Phe-L-Phe ISRP supports involves binding of the non-adsorptive glycerolpropyl groups to the silica surface. While a cursory inspection of the glycolphase coverage data (Table III) implies that the degree of glycolphase coverage is directly proportional to initial specific surface area, this trend is not completely realized. For example, the Zorbax silicas with 350 m<sup>2</sup>/g specific surface area exhibit less specific glycol coverage than the Nucleosil-100 support which has a surface area of only 300 m<sup>2</sup>/g. This discrepancy is seen upon comparison of the Hypersil and Spherisorb silicas as well. If the degree of glycol coverage is truly proportional to the specific surface area of the silica supports, then the coverage expressed relative to the surface area ( $\mu\text{mol}$  glycol groups per square meter of silica surface) should be a constant value which is independent of the type of silica material. For monolayer coverage of glycolphase, this value is around 2  $\mu\text{mol}/\text{m}^2$ <sup>24</sup>. However, as shown in Fig. 4, the glycol coverage per square meter of surface area is not constant for the various silicas used in this study. The smaller pore silicas exhibit less glycol coverage per square meter of surface; indicating that the degree of glycol coverage is more dependent upon pore size than upon surface area. This, most likely, occurs because steric hindrance impedes diffusion of silanizing reagent into some pores of the small pore silicas during derivatization.

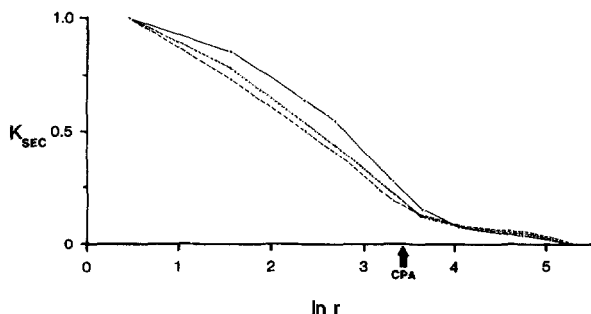


Fig. 3. Pore volume access distributions as determined by inverse size-exclusion chromatography (see Experimental) for ISRP packing, glycolphase silica and the base silica support used by the Regis Chemical Company to produce the packings.  $K_{\text{SEC}}$  is the size-exclusion coefficient and  $r$  is the effective sphere radius (in Å) of polystyrene standards in THF. (—) Silica; (· · · ·) glycolphase silica; (---), ISRP.

TABLE III  
COVERAGE PROPERTIES OF ISRP SUPPORTS

ISRP material	Batch No.	Initial specific surface area* ( $m^2/g$ )	Specific glycolphase coverage ( $\mu mol/g$ )**	Tripeptide coverage***		Cleavage§ (%)	External§§ surface (%)
				Before cleavage ( $\mu mol/g$ )	After cleavage ( $\mu mol/g$ )		
Nucleosil-50	1	500	555	79.9	68.9	14	16
Zorbax	1	350	506	44.6	41.7	7	—
Zorbax	2	350	429	42.1	37.3	11	11
Nucleosil-100	1	300	550	42.3	36.6	14	—
Spherisorb	1	220	373	53.5	43.5	19	—
Spherisorb	2	220	367	73.0	66.5	9	—
Spherisorb	3	220	342	—	—	—	—
Spherisorb	4	220	387	64.3	59.6	7	14
Hypersil	1	180	403	75.9	43.3	43	26

\* Manufacturer's specifications.

\*\* As determined from iodometric titration.

\*\*\* As determined by HPLC analysis of phenylalanine residues released by acid hydrolysis.

§ Percent of dipeptide cleaved from ISRP support.

§§ As determined from pore volume access distributions.

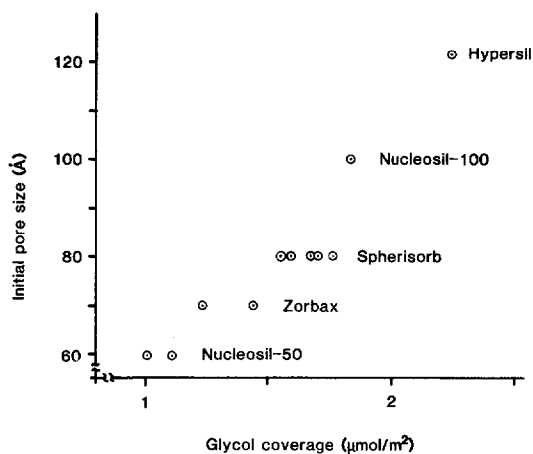


Fig. 4. Dependence of initial nominal pore size on glycolphase coverage in  $\mu\text{mol}$  glycol per square meter of initial surface area (manufacturer's specifications) for various silica supports.

Typical coverage of tripeptide before cleavage ranges from 40–80  $\mu\text{mol}/\text{g}$  for various ISRP supports (Table III). There is no noticeable trend, with regard to initial pore size and surface area, in the degree of tripeptide coverage. This may arise because the surface areas and pore size of the silica supports change upon derivatization with the glycerol groups and the dependence of the new surface areas and pore sizes upon the tripeptide coverage is unrecognizable. It is also possible that the tripeptide coverage is limited by the chemical reaction itself. The reaction time and stoichiometric amount of tripeptide added to the carbonyldiimidazole activated glycolphase support may be the largest factors in determining the coverage of tripeptide. Though observations suggest that lengthening reaction time does yield a small enhancement of tripeptide coverage, to date, no detailed studies have been performed to evaluate this hypothesis.

Percent cleavage of the phenylalanine moieties from the external surface determined from tripeptide coverage analysis before and after enzyme treatment range from 7–43% for the various ISRP packings (Table III). The correlation between the percent cleavage calculated from the coverage analysis and the percent external surface determined from the pore volume access distributions is ambiguous. For the Nucleosil-50 and Zorbax ISRP packings, the percent cleavage, as expected, agrees well with the percent external surface; however, this is not the case for the Spherisorb and Hypersil ISRP packings (Table III). Inhomogeneity in the tripeptide coverage between the internal and external surfaces and/or incomplete enzyme cleavage of the external surfaces could cause these ambiguities. As more ISRP material is produced "in house", the exact correlation between the pore volume access determination of percent external surface and percent cleavage determined from coverage analysis will be made.

The efficiency of cleavage can be assessed from comparison of pore volume access distributions of ISRP supports and their precursor glycolphase silicas. This is exemplified by the pore volume access distributions of the glycolphase and ISRP packings produced by the Regis Chemical Company (Fig. 3). These plots diverge

around the point where the effective sphere radius is equal to that of the carboxypeptidase molecule. For molecules with effective sphere radii *smaller* than that of carboxypeptidase, the fraction of accessible pore volume is *less* for the ISRP support than for the glycolphase packing; while for molecules with effective sphere radii *larger* than that of carboxypeptidase, the fraction of accessible pore volume is *similar* for the two packings. This is expected if the carboxypeptidase effectively cleaves the bulky phenylalanine moieties from the external surface of the tripeptide derivatized support resulting in ISRP material with external pores that are roughly the same size as the external pores of the glycolphase silica.

#### *Chromatographic characterization of ISRP supports*

Relative capacities of the ISRP supports were determined by measuring the capacity factor of the anticonvulsant drug carbamazepine. Capacity factors of the supports ranged from 2.00 to 4.21 (Table II) and demonstrated a strong dependence upon the initial specific surface area of the silica supports. Silicas with large initial surface areas yielded ISRP packings with relatively larger capacity factors for carbamazepine.

The wide range in hydrophobicity of the ISRP supports is important because, in order to minimize conformational changes, denaturation, precipitation and subsequent accumulation of proteins onto the ISRP packings during direct injection of blood serum. The concentration of organic modifier in the mobile phase must remain below 20%<sup>25</sup>. This limits, to some extent, the ability to control retention times of analytes through changing the mobile phase concentration. The availability, however, of ISRP supports with varying degrees of hydrophobicity will offer more control in ISRP drug separation by allowing one to choose the column most suited for a specific separation.

Efficiencies ( $N$ ) of four ISRP chromatographic columns were determined at various chromatographic flow velocities. Plate height *versus* flow velocity plots (Fig.

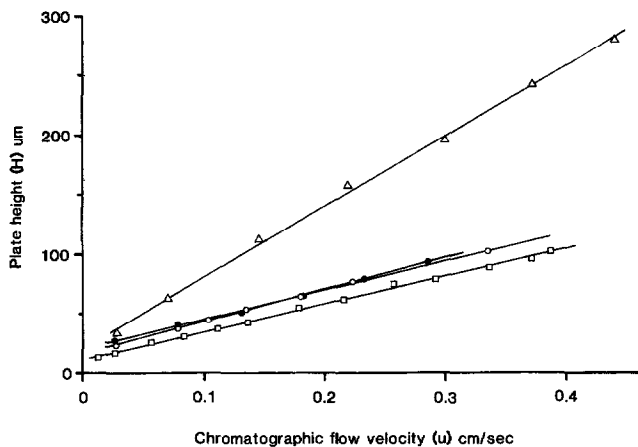


Fig. 5. Plate height *versus* chromatographic flow velocity, relative to carbamazepine of chromatographic columns (15 cm  $\times$  4.6 mm I.D.) packed with various ISRP supports. Mobile phase is 0.1 *M* phosphate-isopropanol-tetrahydrofuran (84:10:6, pH 6.8).  $\Delta$  = Zorbax ISRP, batch No. 2;  $\bullet$  = Nucleosil-50 ISRP, batch No. 1;  $\circ$  = Hypersil ISRP, batch No. 1;  $\square$  = Spherisorb ISRP, batch No. 4.

5) for the Nucleosil-50, Hypersil, and Spherisorb ISRP columns are very similar. The Zorbax ISRP column, however, yields a plate height *versus* flow velocity curve with a slope about twice that of the other ISRP columns. Theoretical plate height terms associated with stagnant mobile phase and stationary phase mass transfer are directly proportional to the flow velocity of the mobile phase. Therefore, the large slope of the plate height *versus* flow velocity plot for the Zorbax ISRP column may indicate that the stagnant mobile phase or stationary phase mass transfer contribution to plate height is large for the Zorbax ISRP material. A possible reason for this is the small pore volume and small median pore diameter (Table II) associated with the Zorbax ISRP packing. A small pore volume leads to a small value of  $k_0$ , which is the ratio of pore volume to interstitial volume in a packed column. The plate height equation according to Horváth and Lin<sup>26</sup> predicts that, for a given system, as  $k_0$  decreases from a value of 1.0, the slope of the plate height *versus* flow velocity plot increases. In addition, packing materials with small pore diameters are suspected of causing low efficiencies in chromatographic columns<sup>7-9</sup>. The Zorbax ISRP material and packed column exhibit the smallest median pore diameter and  $k_0$  value (Table II) of the four evaluated ISRP columns. Therefore, it is possible that the lower efficiencies observed in the Zorbax ISRP support arise from a combination of the low  $k_0$  and small pore size.

## CONCLUSIONS

Three major factors that determine the success of porous ISRP packings for direct injection serum analysis are the ability to exclude proteins from pores without adsorption onto the packing, the capacity for small hydrophobic analytes, and the column efficiency. The effects that the properties of the porous silica supports have upon these three features based on the results of the present investigation are summarized below.

The smallest major protein component in blood plasma is serum albumin. Serum albumin has a molecular weight of 65 600 and its effective sphere radius has been estimated at 40 Å (ref. 1). Because the carboxypeptidase enzyme used to cleave the hydrophobic phase from the external surfaces of ISRP supports is smaller than serum albumin, the carboxypeptidase can reach further into the porous interior of the support allowing cleavage of surfaces inaccessible to the serum albumin<sup>1</sup>. Therefore, the serum albumin will, most likely, have no contact with the hydrophobic partitioning phase and will be excluded, unsorbed from the internal surfaces of the ISRP packing. Because of this, the size of the pores of the silica used to produce ISRP supports is not overly critical with regard to exclusion of serum proteins just as long as the pores are not too large to allow excessive access of the cleavage enzyme to the support surface, and thus leave only a small percentage of internal surface.

Capacity factor measurements of the various ISRP supports produced in this study indicate that capacity is proportional to the surface area of the silica starting material. This allows for variation in the hydrophobicity of ISRP supports by selecting porous silicas with different specific surface areas. In addition pore volume access distributions provide evidence that all the silicas evaluated, even the Hypersil material with an initial nominal pore diameter of 123 Å, result in ISRP supports with enough internal surface to offer adequate capacity for small hydrophobic analytes.

Plate height *versus* flow velocity plots suggest that efficiencies are roughly equivalent for ISRP supports produced from various silicas; however when a combination of small pore volume and small pore diameter exist in a support, such as the Zorbax ISRP packing, poor efficiencies may result.

#### ACKNOWLEDGEMENTS

This investigation was supported by Public Health Service Grant R01-GM34759-01 awarded by the National Institutes of General Medical Sciences, Department of Health and Human Services.

#### REFERENCES

- 1 I. H. Hagestam and T. C. Pinkerton, *Anal Chem.*, 57 (1985) 1757.
- 2 I. H. Hagestam and T. C. Pinkerton, *J. Chromatogr.*, 351 (1986) 239.
- 3 T. Arvidsson, K.-G. Wahlund and N. Daoud, *J. Chromatogr.*, 317 (1984) 213.
- 4 U. Juergens, *J. Chromatogr.*, 310 (1984) 97.
- 5 R. E. Majors, in Cs. Horváth (Editor), *High Performance Liquid Chromatography, Advances and Perspectives*, Vol. 1, Academic Press, New York, 1980, p. 78.
- 6 H. Engelhardt and H. Englass, in Cs. Horváth (Editor), *High Performance Liquid Chromatography, Advances and Perspectives*, Vol. 2, Academic Press, New York, 1980, p. 66.
- 7 A. V. Kiselev, Y. S. Nikitin, I. I. Frolov and Y. I. Iashin, *J. Chromatogr.*, 91 (1974) 187.
- 8 H. Engelhardt and N. Weigand, *Anal Chem.*, 45 (1973) 1149.
- 9 L. R. Snyder and J. J. Kirkland, *Introduction to Modern Liquid Chromatography*, Wiley, New York, 1979, p. 279.
- 10 K. K. Unger, J. N. Kinkel, B. Anspach and H. Giesche, *J. Chromatogr.*, 296 (1984) 3.
- 11 J. J. Kirkland, *J. Chromatogr.*, 125 (1976) 231.
- 12 A. P. Karnaukhov, *Kinet. Katal.*, 12 (1971) 1025.
- 13 A. P. Karnaukhov, *Kinet. Katal.*, 12 (1971) 1235.
- 14 W. Haller, *J. Chem. Phys.*, 42 (1965) 686.
- 15 M. E. van Kreveld and N. van den Hoed, *J. Chromatogr.*, 83 (1973) 111.
- 16 J. H. Knox and H. P. Scott, *J. Chromatogr.*, 316 (1984) 311.
- 17 T. C. Pinkerton and H. I. Hagestam, *U.S. Pat.*, 4,544,485 (1985).
- 18 S. Siggia, *Quantitative Organic Analysis via Functional Groups*, Wiley, New York, 1963, p. 39.
- 19 I. Halász and K. Martin, *Angew. Chem. Int. Ed. Engl.*, 17 (1978) 901.
- 20 R. Nikolov, W. Werner and I. Halász, *J. Chromatogr. Sci.*, 18 (1980) 207.
- 21 F. W. Warren and B. A. Bidlingmeyer, *Anal Chem.*, 56 (1984) 950.
- 22 F. Nevejans and M. Verzck, *Chromatographia*, 20 (1985) 173.
- 23 W. W. Yau, J. J. Kirkland and D. D. Bly, *Modern Size-Exclusion Liquid Chromatography*, Wiley, 1979, p. 114.
- 24 P.-O. Larsson, M. Glad, L. Hansson, M.-O. Mansson, S. Ohlson and K. Mosbach, *Adv. Chromatogr. (N.Y.)*, 21 (1983) 51.
- 25 T. C. Pinkerton, T. D. Miller, S. E. Cook, J. A. Perry, J. D. Rateike and T. J. Szczerba, *BioTechniques*, in press.
- 26 Cs. Horváth and H.-J. Lin, *J. Chromatogr.*, 149 (1978) 43.